Quasars, Blazars, and Gamma Rays

Charles D. Dermer* and Reinhard Schlickeiser

Before the launch of the Compton Gamma Ray Observatory (CGRO), the only source of >100–megaelectron volt (MeV) gamma radiation known outside our galaxy was the quasar 3C 273. After less than a year of observing, 13 other extragalactic sources have been discovered with the Energetic Gamma Ray Experiment Telescope (EGRET) on CGRO, and it is expected that many more will be found before the full sky survey is complete. All 14 sources show evidence of blazar properties at other wavelengths; these properties include high optical polarization, extreme optical variability, flat-spectrum radio emission associated with a compact core, and apparent superluminal motion. Such properties are thought to be produced by those few, rare extragalactic radio galaxies and quasars that are favorably aligned to permit us to look almost directly down a relativistically outflowing jet of matter expelled from a supermassive black hole. Although the origin of the gamma rays from radio jets is a subject of much controversy, the gamma-ray window probed by CGRO is providing a wealth of knowledge about the central engines of active galactic nuclei and the most energetic processes occurring in nature.

A few percent of all galaxies display a bright central nucleus that outshines the billions of stars making up the system. These so-called active galactic nuclei (AGN) are thought to be powered ultimately by the accretion of matter onto central black holes with masses $\gtrsim 10^8$ $M_\odot$ ($M_\odot$ = solar mass) (*1–3*). Some AGN are so distant that their stellar systems, if they exist, cannot be resolved and are therefore referred to as quasi-stellar objects (QSOs). QSOs show broadened redshifted spectral lines and are the earliest coherent structures formed after the Big Bang that are bright enough to be seen through their own radiation. Of the multitude of galaxies and QSOs, only those showing strong radio emission associated with radio jets directed toward us have been reported (*4–12*) as sources in the high-energy gamma-ray sky, implying that the relativistic electrons that produce the radio emission in the jets are also making the gamma rays. The power in gamma rays from these sources often dominates the multiwavelength luminosity. These observations, made at $\gtrsim$100-MeV photon energies with the EGRET, support the unified AGN scenario whereby several different classes of AGN differ primarily in their orientation with respect to the observer (*13, 14*). Observations of AGN at energies of 0.1 to 30 MeV with the Oriented Scintillation Spectrometer Experiment (OSSE) and Compton Telescope (Comptel) on CGRO are also helping to distinguish the different types of AGN. CGRO is providing valuable information about the mechanisms that produce bulk relativistic outflows from supermassive black holes and the processes that energize the nonthermal radio and gamma-ray–emitting particles. These observations will help us determine the composition of the jets and to establish whether they contain substantial mixtures of leptonic antimatter and will also help explain the nature of the diffuse high-energy glow of gamma-ray background radiation discovered by earlier gamma-ray satellite experiments.

C. D. Dermer is in the Department of Space Physics and Astronomy, Rice University, Houston, TX 77251. R. Schlickeiser is at the Max-Planck-Institut für Radioastronomie, Auf dem Hügel 69, D-5300 Bonn 1, Germany.

*To whom correspondence should be addressed, at the E. O. Hulburt Center for Space Research, Naval Research Laboratory, Code 4153, Washington, DC 20375.

Radio-Active AGN and Unified Scenarios

Galaxies, AGN, and QSOs come in many flavors. When viewed at radio frequencies, some emit strongly in the radio band whereas most are radio-quiet. Radio(-loud) galaxies are usually elliptical for reasons that are not fully understood, but that could be related to the fueling of black holes at the dynamical center of galaxies (*15*). The radio emission is thought to be synchrotron emission from relativistic electrons spiraling in a magnetic field. Images of radio galaxies taken at radio frequencies often display two extended radio lobes that point back to a central source. Only a supermassive black hole is thought capable of providing the gyroscopic stability and energy requirements necessary to power these remarkable structures, sometimes reaching to several hundred kiloparsecs from the nucleus.

The hundreds of known radio galaxies divide into two classes according to their morphology and radio luminosity (*16*). Fanaroff-Riley 1 (FR1) radio galaxies are low-luminosity radio galaxies for which the radio brightness peaks around the optical counterpart, that is, in the vicinity of the central source. FR2 galaxies are high-luminosity radio galaxies whose radio emission is brightest near the outer portions of radio lobes, with the radiation often appearing in the form of radio hot spots. The ability of the interstellar medium to disrupt low- and high-luminosity outflows may account for the differences between FR1 and FR2 galaxies. In either case, vast amounts of magnetized plasma must be ejected from the central powerhouse in a highly collimated outflow in order to produce the radiant energy, involving as much as 10^{60} ergs over the lifetime of the source. Figures 1 and 2 show the large-scale radio structure of some representative examples of galaxies belonging to types FR1 and FR2, respectively.

Some 5 to 10% of optically selected QSOs are radio-loud and are referred to as quasars (quasi-stellar radio sources). Being a subset of QSOs, they have redshifted spectral lines emitted by sources thought to be cosmologically distant, because an expanding cosmology provides the most compelling explanation for the origin of the redshifted lines. At such distances, only very luminous radio sources can be detected. Many display compact radio cores with very little extended emission, although fainter extended radio halos are sometimes observed. Quasars generally have more compact cores and more luminous radio emission than radio galaxies at the same redshift. The increased prominence of the compact, variable, polarized synchrotron cores in quasars is generally

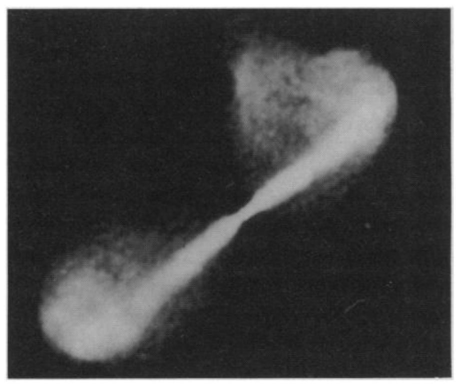

Fig. 1. An example of an FR1 source, the radio galaxy 3C 296 (*63*), which has a radio luminosity of $\approx 5 \times 10^{41}$ erg s^{-1}. [Courtesy J. P. Leahy] Note the plumed nature of the two opposing jets. [Adapted from (*63*), with permission of Macmillan Magazines, London, copyright 1992]

Fig. 2. An example of an FR2 source, the famous radio galaxy Cygnus A, with a radio luminosity of $\approx 10^{45}$ erg s^{-1}. The radio emission is brightest in hot spots at lobes some 60 kpc from the central source. Gamma rays with energies >100 MeV evidently come from sources with radio jets aligned toward us. [Courtesy C. Carilli, R. Perley, and J. Dreher]

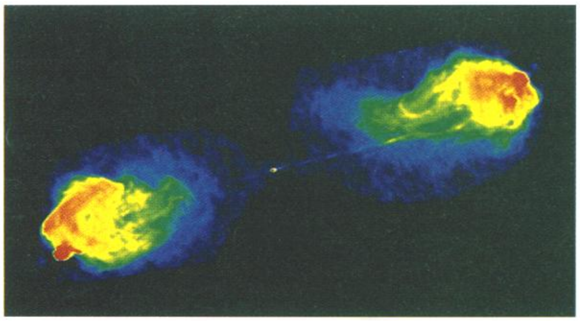

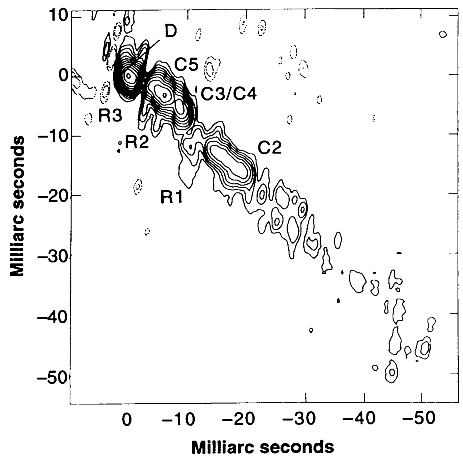

Fig. 3. Radio map of the quasar 3C 273 at 5 GHz (*64*) made with the high-resolution Very Long Baseline Interferometer. By charting the angular movement of the various components (labeled C2, C3, . . .) over many years, and determining the distance from the redshift of spectral lines, SL motion was established. 3C 273 was the first quasar discovered and the first from which gamma rays >100 MeV were detected. Note that 1 milliarc sec corresponds to a distance of only ~2 pc. [Adapted from J. A. Zensus *et al.* (*64*), with permission of Macmillan Magazines, London, copyright 1988]

attributed to the orientation of the observer and the beaming of the emission. The spectrum of the radio emission over a limited frequency band can be represented by a power law function

$$S(\nu) \propto \nu^{-\alpha} \quad (1)$$

where $S(\nu)$ is measured in janskys (Jy = 10^{-26} W m^{-2} Hz^{-1}). The frequencies used in most radio studies lie between 100 MHz and 30 GHz.

A clear contrast is seen between the properties of flat-spectrum radio quasars (FSRQs; $\alpha \leq 0.5$) and steep-spectrum radio quasars (SSRQs; $\alpha > 0.5$). The FSRQs tend to have higher optical polarization and more compact cores, whereas the SSRQs generally display more extended emission (*17*). FSRQs are more likely to be classified as optically violent variables (OVVs), which are those quasars showing dramatic optical variability (factor of 2 within a week) and a highly polarized optical continuum. Moreover, unlike SSRQs, FSRQs often show superluminal (SL) motion (*18*), wherein the velocities of radio-emitting knots emerging from compact radio cores, measured transverse to the line of sight, appear to exceed the speed of light.

Apparent transverse SL motion is a relativistic illusion related to the Lorentz transformation of the time interval of radiating material moving at relativistic speeds. It was discovered by charting the motions of outflowing radio features over many years with milliarc second–resolution radio interferometry (*19*). The possibility of SL motion from quasars was in fact predicted more than a decade before it was discovered (*20*). Figure 3 shows a radio image of the quasar 3C 273, whose outflowing knots display SL motion. In addition to FSRQs, another class of radio sources, the BL Lac objects, also commonly exhibit SL motion (*21*). These compact radio sources are not properly classified as quasars or QSOs because they have a nearly featureless optical continuum with extremely weak emission lines and are sometimes found to be associated with low-redshift elliptical galaxies. Like the OVVs, they also display strong optical polarization and rapid optical variability. Table 1 summarizes the properties of the various types of active galaxies discussed in this article.

The blazar category unites compact radio sources having continuum characteristics common to the OVVs and BL Lac objects, including SL motion. Blazars must therefore be those extragalactic radio sources whose jets are closely aligned along our observing direction. Sources whose jet axes are inclined at larger angles to us appear as SSRQs or radio galaxies. The relativistic beaming of the emission, which amplifies the radiation intensity by orders of magnitude, complicates the relationships among the different types of sources, but one of the most successful unification schemes links FR2s, SSRQs, and FSRQs on the one hand (*22*) and FR1s and BL Lac objects on the other (*23, 24*), with the jet axes of the radio galaxies being most nearly perpendicular to the line of sight. Another proposes to unify the lower redshift BL Lac objects with the higher redshift FSRQs through separate luminosity evolution of beamed and isotropic components (*25*), and still another identifies radio galaxies as quasars whose central nuclei are obscured from our view by an opaque torus of dust (*26*).

Nature of the Gamma-Ray AGN Discovered by EGRET

EGRET works by converting an incoming gamma ray into an electron-positron pair and following the paths of these particles through a multilevel spark chamber to determine arrival direction (*27, 28*). The total energy of the gamma ray is measured with a scintillation calorimeter. The half-width half-maximum EGRET field of view is ~20°, and CGRO nominally views a given target for 2 weeks per pointing. The full sky survey will therefore require about 30 separate pointings, of which ~65% has been completed as of May 1992.

EGRET images strong sources to within 5 to 10 arc min. For a conservative source localization error box of 1/2° by 1/2°, source confusion will not be a serious problem if there are fewer than several candidate sources per square degree. Some 8000 AGN are known (*29*), representing ~0.2 AGN per square degree on average. Source identification should thus be fairly unambiguous if extragalactic gamma-ray sources indeed arise from AGN rather than from normal galaxies or clusters of galaxies. One can test this assumption by looking for evidence of gamma-ray emission from local galaxies or clusters.

The 14 extragalactic sources detected by EGRET are arranged in Table 2 in order of increasing redshift. The redshifts of two (4C 15.05 and 0528 + 134) are uncertain, and the redshift of another (0716 + 714) is unknown. The gamma-ray AGN appear five times in Impey's list (*30*) of 25 known SLs and twice in his list of possible SLs. Of the possible SLs, 0716 + 714 would be SL if its redshift $z \geq 0.28$, which is likely in view of its stellar optical appearance (*31*). The values of the 2.7-GHz flux densities listed in Table 2 show that all gamma-ray AGN are fairly strong radio sources, although it is interesting that the closest source, Mkn 421, is also the weakest radio source. Four of the fourteen, Mkn 421, PKS 0537 − 441, PKS 0235 + 164, and 0716 + 714, are classified as BL Lac objects because of their weak emission lines. In fact, Mkn 421 is the second closest BL Lac object known and, being at the center of a luminous elliptical galaxy, displays extended radio emission (*21*).

Twelve of the 14 gamma-ray AGN are found in the Impey-Tapia sample (*32*) of 140 quasars brighter than 1.5 Jy at 5 GHz. The missing two, Mkn 421 and 0716 + 714, are both dimmer than 1.5 Jy. Eleven

Table 1. Types of active galaxies, abbreviations, and a brief description of their defining properties.

Type	Abbreviation	Properties
Active galactic nucleus	AGN	Extragalactic source with a variable bright central nucleus
Quasi-stellar object	QSO	Unresolved extragalactic source with broad spectral lines
Quasar	QSR	Radio-loud QSO*
Fanaroff-Riley 1 radio galaxy	FR1	Low-radio-luminosity radio galaxy; emission peaked near central source
Fanaroff-Riley 2 radio galaxy	FR2	High-radio-luminosity radio galaxy; emission brightest at lobes or hot spots far from central source
Flat-spectrum radio quasar	FSRQ	Quasar with radio spectral index $\alpha \leq 0.5$ over a specified energy range (see Eq. 1)
Steep-spectrum radio quasar	SSRQ	Quasar with radio spectral index $\alpha > 0.5$
Optically violent variable	OVV	AGN with dramatic optical variability and highly polarized optical continuum
Superluminal	SL	Source with features sometimes appearing to move faster than the speed of light
BL Lacertae object	BL Lac	AGN with featureless optical continuum and weak emission lines
Blazar		AGN with strong optical polarization; rapid optical variability; flat-spectrum radio emission

*This definition is not universally accepted. Often QSOs, whether radio-loud or radio-quiet, are referred to as quasars.

of the gamma-ray AGN are found in the Wall-Peacock (WP) catalog (*33*) of 233 extragalactic radio sources brighter than 2 Jy at 2.7 GHz. These catalogs, made at relatively high radio frequencies, preferentially select FSRQs as compared to the Cambridge 3CR catalog, for example, which is biased toward SSRQs because of its lower survey frequency (178 MHz). The WP catalog lists 56 FSRQs and 29 SSRQs as defined by their 2.7 to 5.0 GHz spectral index. Nine of the 11 gamma-ray AGN found in the WP catalog are classified as FSRQs. Of the other two, 4C 15.05 is presumed to be a galaxy and CTA 102 is technically an SSRQ ($\alpha = 0.67$), although Padovani and Urry (*22*) reclassify this object as an FSRQ because of its high optical polarization and apparent SL motion.

Optical brightness is not a good discriminant of gamma-ray–bright AGN. Only 3C 273 is found among the 114 objects in the Bright Quasar Survey (*34*), which explored the sky outside a 30° band centered on the galactic plane with an effective limiting visual magnitude $B = 16.16$. We also find that gamma-ray AGN are not strongly correlated with x-ray–selected AGN. Of the 842 galactic and extragalactic sources appearing in the High Energy Astrophysical Observatory- A-1 source catalog (*35*), which is 90% complete above 1.5 μJy at 5 keV, only 3C 273, Mkn 421, and possibly 0716 + 714, are identified. The gamma-ray quasars do, however, show up on lists of extragalactic x-ray sources that are radio-selected. For example, seven gamma-ray AGN are found among the 61 Einstein x-ray sources associated with core-dominated radio sources (*36*).

Table 2. Active galactic nuclei reported to be 100-MeV gamma-ray sources of 11 May 1992. Data for redshift z, S(2.7 GHz), and α(2.7 to 5 GHz) are from (*33*), except for Mkn 421, 0235 + 164, and 0716 + 714, for which data are from (*29*) and (*31*).

Name	Galactic location*	Type†	z	S(2.7 GHz) (Jy)	α(2.7 to 5 GHz)
Mkn 421	1101 + 384	BL Lac	0.031	0.57	−0.32
3C 273	1226 + 02	SL	0.158	38.9	−0.05
3C 279	1253 − 05	OVV/SL	0.538	11.2	−0.59
3C 454.3	2251 + 158	SL	0.86	10.0	−1.37
PKS 0537 − 441	0537 − 441	BL Lac	0.894	3.84	0.02
PKS 0420 − 014	0420 − 014		0.915	2.15	0.01
PKS 0235 + 164	0235 + 164	BL Lac/SL	0.94	1.94	−0.59
PKS 0208 − 512	0208 − 512		1.003	3.56	0.17
CTA 102	2230 + 11	SL	1.037	5.3	0.67
4C 15.05	0202 + 149		1.202‡	3.0	0.43
4C 38.41	1633 + 38		1.814	2.53	−0.78
OG 147	0528 + 134		1.928‡	2.97	−0.43
0836 + 710	0836 + 710	SL	2.16	3.15	0.39
0716 + 714	0716 + 714	BL Lac/SL(?)	?	0.98	−0.22

*Given by right ascension and declination in Julian 1950 coordinates. †All except Mkn 421, 4C 15.05, and CTA 102 are FSRQs (see text). ‡Redshift uncertain.

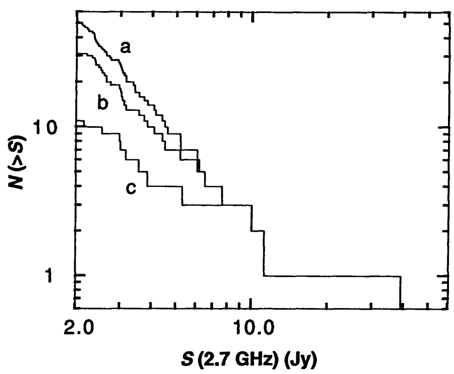

Fig. 4. The size distribution of FSRQs (curve a) with 2.7-GHz flux density > S found in the Wall-Peacock catalog (*33*). Also shown are (curve b) the size distribution of FSRQs in the Wall-Peacock catalog located within 20° of the EGRET pointing directions as of VP 21 ending 5 March 1992, and (curve c) the size distribution of the gamma-ray AGN identified with FSRQs, covering source identifications through VP 21.

Thus we see that the reported gamma-ray AGN are clearly associated with compact core, flat-spectrum radio sources, in particular, those showing evidence for SL motion. Moreover, there is a correlation between radio brightness and gamma-ray brightness, because the brighter flat-spectrum quasars in the 2-Jy survey tend to be the AGN identified at gamma-ray energies. This is apparent from Fig. 4, where the radio-flux size distributions of gamma-ray AGN and FSRQs in the WP catalog are plotted. Although the gamma-ray sky survey is not yet complete, the apparent correlation between gamma-ray brightness and radio brightness suggests that the most likely candidate gamma-ray AGN sources are radio-bright FSRQs, particularly those showing SL motion. From the remaining 47 FSRQs in the WP catalog, we predict that 0212 + 73, 3C 84 (NGC 1275), 3C 216, 4C 39.25, 3C 120, 4C 73.18, BL Lac, and 3C 446 are the most probable sources of 100-MeV gamma radiation.

Source Models

Considering the thousands of known AGN, it is remarkable that the ones reported as >100-MeV sources are associated overwhelmingly with blazar-type radio sources. By contrast, three extragalactic sources of >0.5-MeV flux, in addition to 3C 273, were known before the launch of CGRO (*37, 38*). Two are radio-quiet AGN with broad optical and ultraviolet emission lines known as Seyfert 1s (NGC 4151, MCG 8-11-11) and one is a radio galaxy (Cen A). Emission near 200 keV was also detected

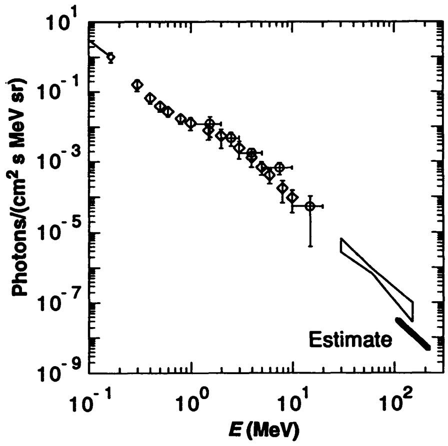

Fig. 5. Data points show measurements (*53–56*) of the diffuse high-energy extragalactic background radiation. The solid curve shows the upper limit to the high-energy contribution from extragalactic radio sources obtained through the simple estimate performed here. Another class of sources or a diffuse component may be necessary to account for the bulk of the emission.

from the irregular galaxy NGC 1275, usually identified as a BL Lac object. For completeness, we also mention the unconfirmed detection (*39*) of Cen A at ultrahigh energies ($>10^{12}$ eV).

To date, EGRET has reported detections of neither NGC 4151 nor NGC 1275, though both were pointing targets and NGC 1275 is a likely source according to the considerations mentioned above. OSSE observations show that the luminous hard x-ray flux of NGC 4151 cuts off very sharply below 1 MeV (*40*). The x-rays are generally attributed to matter accreting onto a supermassive black hole in a disk-like geometry. The absence of significant megaelectron volt emission has been attributed to an upper limit on the electron temperature imposed by the onset of pair production in compact systems (*38*). But even if 100-MeV gamma rays were created near the central source by, for example, pion production in proton-ion collisions, these photons would be severely attenuated by $\gamma - \gamma$ pair production (*41*).

The evidence from CGRO clearly implies that the high-energy gamma rays originate from strongly beamed sources. Beaming of the emission is also suggested on energetics grounds: if the emission were instead isotropic, one must find a process in nature that channels the bulk of the radiant energy into high-energy photons. Thus it appears that quasi-isotropic models involving, for example, two-temperature accretion disks (*42*) or quasi-spherical neutron outflow (*43*) will have a difficult task accounting for the EGRET observations. Models with gamma-ray production in the jets seem required, yet even these have difficulties.

One of the earliest models proposed for the 100-MeV emission from 3C 273 involved pion production from collisions of protons with matter in the intergalactic gas near the outer lobes of the radio jet (*44*). We now know that there can be rapid variability in the gamma-ray emission of 3C 279 (*6*), which seems to require an emission site less than about a light-week away from the central black hole for 3C 279, although there could be more slowly varying emission produced at greater distances in the jets of 3C 273, 3C 279, or the other gamma-ray AGN. Secondary pion production could be produced near the base of the jet if there were an ambient plasma outflow with which the high-energy protons and ions interact. But such a spectrum would be expected to exhibit a feature near 70 MeV, which would be blueshifted to higher energies by the relativistic motion of the jet. No such feature is observed in the spectrum of 3C 279, although a detection would strongly argue in favor of such models.

Another class of models proposed for the gamma radiation from extraglactic radio sources is the synchrotron self-Compton process (*45, 46*). Here the same electrons that produce the radio emission rescatter these low-energy photons to higher energies through the Compton process. Such emission must be formed; indeed, upper limits to the observed x-ray emission have been used to predict that the source National Radio Astronomy Observatory 140 displays SL motion, because higher velocity relativistic outflow in SL sources limits the level of self-Compton x-ray emission (*47*). But the power-law gamma-ray spectrum observed from 3C 279 is difficult to model with the simplest version of this model, because rather curved Comptonized synchrotron spectra are obtained unless the electron spectrum is a power law over a large energy range. This model also predicts that radio flares should accompany gamma-ray flares, although inhomogeneous synchrotron self-Compton models (*48*) can produce a wider variety of spectra and time histories that can fit the data.

We favor a model (*49*) in which electrons are accelerated to high energies near the base of the radio jet in the vicinity of the supermassive black hole, in accord with the 1- to 2-day variability time scale of the gamma-ray flare from 3C 279. Low-energy photons radiated by the accretion disk surrounding the supermassive black hole will intercept the jet and be upscattered to very high energies (*50*). Because the scattered radiation is highly beamed, there is no difficulty in satisfying the energy requirements of the gamma-ray AGN. At larger distances from the central black hole, nonthermal electrons in the jet scatter accretion disk photons or rescatter the Comptonized radiation coming almost directly from behind. Scattering far from the central source produces the slowly varying or quiescent emission. An unusual property of this geometry is that the emission is scattered in a hollow cone enhanced in a direction that favors detection of SL radio sources (*51, 52*). This may explain the prevalence of SL sources among the gamma-ray AGN.

Gamma-Ray AGN and the Extragalactic Gamma-Ray Background

The limited imaging capability of hard x-ray and gamma-ray telescopes prevents us from knowing whether the extragalactic background radiation at high energies arises from genuinely diffuse emitters distributed throughout the observable universe or from a superposition of discrete sources. The best we can do is subtract off the contributions of sources as they become known and determine whether the residual emission still requires a diffuse source contribution.

The extragalactic gamma-ray background measured by CGRO has not yet been reported, but earlier measurements (*53–56*), plotted in Fig. 5, show a power-law behavior at energies <1 MeV and >10 MeV. A feature near 3 MeV in the gamma-ray background is also seen. Many models for the origin of this radiation have been suggested. Stecker (*57*) proposed a diffuse emission model in which the gamma-ray background arises in a baryon symmetric cosmology from diffuse matter-antimatter annihilation early in the history of our universe, when $z \leq 100$. The 3-MeV bump is thought to represent redshifted π^0 decay radiation formed in proton-antiproton annihilation, which peaks near 70 MeV when originally formed. Many other models (*37, 58*) have considered whether the gamma-ray background radiation arises from the superposition of emission from AGN and quasars, which appeared likely because the 100-MeV spectral slopes of 3C 273 ($\alpha \cong 2.5$) and the background radiation ($\alpha \cong 2.35$) are in rough accord. Furthermore, the origin of the 3-MeV bump can be ascribed to transient megaelectron volt bumps observed in the spectra of such Seyfert galaxies as NGC 4151 and MCG 8-11-11.

The identification of gamma-ray AGN as a class permits a much more reliable estimate of the discrete source contribution. A complete model requires an integration over the source density and luminosity function throughout cosmic time, which cannot yet be reliably estimated until the gamma-ray flux values are reported. Figure 4 shows, however, that gamma-ray–bright AGN are associated with radio-bright quasars. Making the *ansatz* that they are linearly related, we can sum the integrated contribution to the gamma-ray background emitted by extragalactic radio sources using the expression

$$\Phi(>100\ \text{MeV})(\text{cm}^{-2}\ \text{s}^{-1}\ \text{sr}^{-1}) = \int_0^\infty dS\ S\left(\frac{dN}{dSd\Omega}\right)\left(\frac{S_{\gamma,\text{thr}}}{S_{\text{radio,thr}}}\right)\eta \qquad (2)$$

where N is the number of radio sources, Ω is the solid angle, and η is a correction factor for the gamma-ray duty cycle of a radio source as well as for the fraction of radio sources that are gamma-ray emitters. From Fig. 4, we see that the EGRET gamma-ray threshold $S_{\gamma,\text{thr}} \approx 10^{-7}$ photons (>100 MeV) $\text{cm}^{-2}\ \text{s}^{-1}$ corresponds roughly to the radio threshold $S_{\text{radio,thr}} \approx 3$ Jy.

We perform the integration in Eq. 2 using $dN/dSd\Omega$, the radio flux size distribution per steradian, given for 54,579 radio sources with flux densities between 25 mJy and 10 Jy (*59*). In the best possible case, all radio sources emit >100 MeV gamma rays all the time, so we let $\eta = 1$. This exercise gives $\Phi(>100\ \text{MeV}) \approx 3 \times 10^{-6}$ photons (>100 MeV) $\text{cm}^{-2}\ \text{s}^{-1}\ \text{sr}^{-1}$, a factor of 5 less than the value $1.3 \pm 0.5 \times 10^{-5}$ photons (>100 MeV) $\text{cm}^{-2}\ \text{s}^{-1}\ \text{sr}^{-1}$ reported by Thompson and Fichtel (*56*).

We have used the most optimistic assumptions possible in our estimate and still fall short by a large factor. This interesting result therefore argues against the conclusion that radio sources are the sole contributors to the gamma-ray background, as additionally suggested by the fact that the spectral slopes reported for 3C 279 (*5*) and the other newly discovered gamma-ray AGN fail to match the slope of the gamma-ray background spectrum (in contrast to the earlier rough agreement for 3C 273). It is possible that our linear scaling is incorrect and that weaker radio sources will tend to be relatively gamma-ray brighter than stronger radio sources, but this is not implied by Fig. 4. More likely, perhaps, is the possibility that Seyfert galaxies and radio-quiet extragalactic sources will prove to be sources of >100-MeV gamma rays, although their flux as yet falls below the EGRET threshold. But neither can a diffuse origin of a large fraction of the emission be discounted.

One test that could implicate blazars as a major contributor to the gamma-ray background is the following: If we are indeed looking almost directly down an outflowing relativistic jet of material, then electrons and positrons in the jet could annihilate, forming 0.511-MeV annihilation radiation in the comoving fluid frame (*49*). In the observer's frame, this emission would be broadened and blueshifted by the motion of the jet; in addition, there would be some redshifting from universal expansion. Superposition of many such sources could produce the 3-MeV bump in the gamma-ray background. Detection of a time-varying annihilation feature in the spectra of gamma-ray AGN with the OSSE or Comptel experiments on CGRO would have enormous ramifications on source models, because production of electron-positron pairs is usually thought to require compact regions near the central black hole (*3*). The mechanism for explaining the relativistic speeds of jets (*60*), which is at present poorly understood, depends strongly on the composition of the jets. An electron-positron jet may support a Compton rocket model (*61*) with radiation pressure accelerating nonthermal pair plasma to bulk relativistic energies.

The results from CGRO also promise to radically alter our understanding of the origin of cosmic rays, which are the highest energy particles known. It is now clear from the EGRET data that extragalactic radio jets can energize particles to high energies, but could they be the sources of cosmic rays with energies $>10^{15}$ eV, or even $\geq 10^{20}$ eV? Ultrahigh-energy gamma-ray telescopes which, unlike CGRO, are ground-based because they detect Cerenkov radiation or shower particles from high-energy photons and particles entering the atmosphere, can now be alerted to look at quasar jets during periods of intense gamma-ray flaring. A victory can already be claimed through the recent detection (*62*) of Mkn 421 at 10^{12}-eV energies by the Whipple Observatory. Perhaps quasars and blazars will also produce detectable neutrino emissions coincident with the gamma-ray flares. Although the meaning of the new results being returned from the Compton Observatory is still unclear, we can be sure that our changing knowledge of the landscape of the universe, containing supermassive black holes, enormous jets, and powerful accelerators, will continue to amaze.

Note added in proof: Two new extragalactic sources of >100-MeV gamma rays, 0454 − 463 and 1606 + 106, have been reported since this article was written. Both are distant quasars with $z > 0.8$. The source 0454 − 463 is an FSRQ and appears in the WP catalog with a 2.7-GHz flux density of 2.36 Jy, whereas the flux density of 1606 + 106 is less than 2 Jy.

REFERENCES AND NOTES

1. M. C. Begelman, R. D. Blandford, M. J. Rees, *Rev. Mod. Phys.* **56**, 255 (1984).
2. L. Woltjer, in *Active Galactic Nuclei*, T. L.-L. Courvoisier and M. Mayor, Eds. (Springer-Verlag, New York, 1990), pp. 1–55.
3. M. J. Rees, *Annu. Rev. Astron. Astrophys.* **22**, 471 (1984).
4. G. F. Bignami *et al.*, *Astron. Astrophys.* **93**, 71 (1981).
5. R. C. Hartman *et al.*, *Astrophys. J.* **385**, L1 (1992).
6. Compton Observatory/EGRET Team, G. Kanbach *et al.*, *Int. Astron. Union Circ. 5431* (17 January 1991).
7. Compton Observatory/EGRET Team, C. E. Fichtel *et al.*, *Int. Astron. Union Circ. 5460* (28 February 1992).
8. Compton Observatory/EGRET Team, P. F. Michelson *et al.*, *Int. Astron. Union Circ. 5470* (10 March 1992).
9. Compton Observatory/EGRET Team, R. C. Hartman *et al.*, *Int. Astron. Union Circ.* **5477** (18 March 1992).
10. Compton Observatory/EGRET Team, R. C. Hartman *et al.*, *Int. Astron. Union Circ. 5519* (11 May 1992).
11. R. A. Kroeger *et al.*, paper presented at the 1992 Joint April Meeting of the American Physical Society, Washington, DC, 23 April 1992.
12. D. J. Morris *et al.*, *ibid.*
13. R. D. Blandford and M. J. Rees, in *Pittsburgh Conference on BL Lac Objects*, A. M. Wolfe, Ed. (Pittsburgh Univ. Press, Pittsburgh, 1978), p. 328.
14. P. A. G. Scheuer and A. C. S. Readhead, *Nature* **277**, 182 (1979).
15. R. D. Blandford, in *Active Galactic Nuclei*, T. L.-L. Courvoisier and M. Mayor, Eds. (Springer-Verlag, New York, 1990), pp. 161–275.
16. B. L. Fanaroff and J. M. Riley, *Mon. Not. R. Astron. Soc.* **167**, 31P (1974).
17. C. D. Impey, C. R. Lawrence, S. Tapia, *Astrophys. J.* **375**, 46 (1991).
18. T. J. Pearson, A. C. S. Readhead, P. D. Barthel, in *Superluminal Radio Sources*, J. A. Zensus and T. J. Pearson, Eds. (Cambridge Univ. Press, New York, 1987), pp. 94–103.
19. R. W. Porcas, *ibid.*, pp. 12–25.
20. M. J. Rees, *Nature* **211**, 468 (1966).
21. R. L. Mutel, in *Parsec-Scale Radio Jets*, J. A. Zensus and T. J. Pearson, Eds. (Cambridge Univ. Press, New York, 1990), pp. 98–109.
22. P. Padovani and C. M. Urry, *Astrophys. J.* **387**, 449 (1992).
23. I. W. A. Browne, *Mon. Not. R. Astron. Soc.* **204**, 23P (1983).
24. C. M. Urry, P. Padovani, M. Stickel, *Astrophys. J.* **382**, 501 (1991).
25. F. Vagnetti, E. Giallongo, A. Cavaliere, *ibid.* **368**, 366 (1991).
26. P. D. Barthel, *ibid.* **336**, 606 (1989).
27. G. Kanbach *et al.*, in *Proceedings of the Gamma Ray Observatory Science Workshop*, W. N. Johnson, Ed. [National Aeronautics and Space Administration (NASA), Greenbelt, MD, 1989], pp. 2-1 to 2-10.
28. D. A. Kniffen, in *Fourteenth Texas Symposium on Relativistic Astrophysics*, E. J. Fenyves, Ed. (New York Academy of Sciences, New York, 1989), pp. 482–496.
29. M.-P. Véron-Cetty and P. Véron, in *European Southern Observatory Scientific Report No. 10* (European Southern Observatory, Garching bei München, Germany, 1991).
30. C. D. Impey, in *Superluminal Radio Sources*, J. A. Zensus and T. J. Pearson, Eds. (Cambridge Univ. Press, New York, 1987), pp. 233–250.
31. M. Stickel, P. Padovani, C. M. Urry, J. W. Fried, H. Kühr, *Astrophys. J.* **374**, 431 (1991).
32. C. D. Impey and S. Tapia, *ibid.* **354**, 124 (1990).
33. J. V. Wall and J. A. Peacock, *Mon. Not. R. Astron. Soc.* **216**, 173 (1985).
34. H. Tananbaum, Y. Avni, R. F. Green, M. Schmidt, G. Zamorani, *Astrophys. J.* **305**, 57 (1986).
35. K. S. Wood *et al.*, *Astrophys. J. Suppl. Ser.* **56**, 507 (1984).
36. D. M. Worrall and B. J. Wilkes, *Astrophys. J.* **360**, 396 (1990).
37. L. Bassani and A. J. Dean, *Space Sci. Rev.* **35**, 367 (1983).
38. C. D. Dermer, in *Fourteenth Texas Symposium on Relativistic Astrophysics*, E. J. Fenyves, Ed. (New York Academy of Sciences, New York, 1989), pp. 513–521.
39. J. E. Grindlay *et al.*, *Astrophys. J.* **197**, L9 (1975).
40. J. D. Kurfess, personal communication.
41. R. J. Protheroe, A. Mastichiadis, C. D. Dermer, *Astroparticle Phys.*, in press.
42. J. A. Eilek and M. Kafatos, *Astrophys. J.* **271**, 804 (1983).
43. P. M. Giovanoni and D. Kazanas, *Nature* **345**, 319 (1990).
44. P. Morrison, D. Roberts, A. Sadun, *Astrophys. J.* **280**, 483 (1984).
45. A. P. Marscher, *ibid.* **235**, 386 (1980).
46. A. Königl, *ibid.* **243**, 700 (1981).

47. A. P. Marscher and J. J. Broderick, *ibid.* **255**, L11 (1982).
48. L. Maraschi, G. Ghisellini, A. Celotti, in *Testing the AGN Paradigm*, S. S. Holt, S. G. Neff, C. M. Urry, Eds. (American Institute of Physics, New York, 1992), p. 439.
49. C. D. Dermer and R. Schlickeiser, in preparation.
50. F. Melia and A. Königl, *Astrophys. J.* **340**, 162 (1989).
51. C. D. Dermer, R. Schlickeiser, A. Mastichiadis, *Astron. Astrophys.* **256**, L27 (1992).
52. ______, in *The Compton Observatory Science Workshop*, C. R. Shrader, N. Gehrels, B. Dennis, Eds. (NASA Scientific and Technical Information Program, Washington, DC, 1992), pp. 328–334.
53. R. Kinzer, W. Johnson, J. Kurfess, *Astrophys. J.* **222**, 370 (1978).
54. V. Schönfelder, F. Graml, F. P. Penningsfeld, *ibid.* **240**, 330 (1980).
55. J. I. Trombka *et al.*, *ibid.* **212**, 925 (1977).
56. D. J. Thompson and C. E. Fichtel, *Astron. Astrophys.* **109**, 352 (1992).
57. F. W. Stecker, *Astrophys. J.* **212**, 60 (1977).
58. G. F. Bignami, C. E. Fichtel, R. C. Hartman, D. J. Thompson, *ibid.* **232**, 649 (1979).
59. P. C. Gregory and J. J. Condon, *Astrophys. J. Suppl. Ser.* **75**, 1011 (1991).
60. M. A. Abramowicz, in *Extragalactic Radio Sources: from Beams to Jets*, in press.
61. A. Y. S. Cheng and S. L. O'Dell, *Astrophys. J.* **251**, L49 (1981).
62. M. Punch *et al.*, *Nature*, **358**, 477 (1992).
63. S. Garrington, *ibid.* **355**, 771 (1992).
64. J. A. Zensus, L. B. Baath, M. H. Cohen, G. D. Nicolson, *ibid.* **334**, 410 (1988).
65. Comments from and discussions with C. D. Impey, C. E. Fichtel, R. C. Hartman, G. Kanbach, J. D. Kurfess, A. P. Marscher, J. R. Mattox, and D. J. Thompson are gratefully acknowledged. The work of C.D.D. is supported by the Gamma Ray Observatory Guest Investigator Program through NASA grant NAG 5-1547.

Galileo Encounter with 951 Gaspra: First Pictures of an Asteroid

M. J. S. Belton, J. Veverka,* P. Thomas, P. Helfenstein, D. Simonelli, C. Chapman, M. E. Davies, R. Greeley, R. Greenberg, J. Head, S. Murchie, K. Klaasen, T. V. Johnson, A. McEwen, D. Morrison, G. Neukum, F. Fanale, C. Anger, M. Carr, C. Pilcher

Galileo images of Gaspra reveal it to be an irregularly shaped object (19 by 12 by 11 kilometers) that appears to have been created by a catastrophic collisional disruption of a precursor parent body. The cratering age of the surface is about 200 million years. Subtle albedo and color variations appear to correlate with morphological features: Brighter materials are associated with craters especially along the crests of ridges, have a stronger 1-micrometer absorption, and may represent freshly excavated mafic materials; darker materials exhibiting a significantly weaker 1-micrometer absorption appear concentrated in interridge areas. One explanation of these patterns is that Gaspra is covered with a thin regolith and that some of this material has migrated downslope in some areas.

On 29 October 1991, the Galileo spacecraft flew past 951 Gaspra at a distance of 1600 km and obtained the first close-up views of an asteroid. Because Galileo's high-gain antenna has not yet been deployed, it was planned to play back all of the Gaspra data to Earth using the smaller, low-gain antenna in November 1992 when the spacecraft returns for its final Earth flyby on its way to Jupiter. However, analysis of telemetry and optical navigation pictures taken during the weeks before encounter demonstrated that knowledge of the spacecraft and asteroid geometry had reached such high precision that the asteroid could be located in individual frames of the Solid State Imaging (SSI) camera. As a result, it was feasible to play back the relevant portions of four images at the available 40 bits per second data rate in early November 1991. These four images were taken in four different spectral bands (0.40, 0.56, 0.89, and 0.99 μm) within an interval of 25 s and represent the highest spatial resolution color data gathered by Galileo during its 8-km/s flyby. They were obtained at an average range of 16,065 km some 36 minutes before closest encounter. In this article we summarize the major conclusions about the current state and past evolution of Gaspra that can be inferred from these data.

M. J. S. Belton is with the National Optical Astronomy Observatories, Tucson, AZ 85719.
J. Veverka, P. Thomas, P. Helfenstein, D. Simonelli are in the Department of Astronomy, Cornell University, Ithaca, NY 14853.
C. Chapman is with the Planetary Science Institute, Tucson, AZ 85719.
M. E. Davies is with RAND, Santa Monica, CA 90406.
R. Greeley is in the Department of Geology, Arizona State University, Tempe, AZ 85287.
R. Greenberg is with the Lunar and Planetary Laboratory, University of Arizona, Tucson, AZ 85721.
J. Head and S. Murchie are in the Department of Geology, Brown University, Providence, RI 02912.
K. Klaasen and T. V. Johnson are with the Jet Propulsion Laboratory, California Institute of Technology, Pasadena, CA 91109.
A. McEwen is with the U.S. Geological Survey, Flagstaff, AZ 86001.
D. Morrison is with the NASA/Ames Research Center, Moffett Field, CA 94035.
G. Neukum is with the Deutsche Forschungsanstalt für Luft und Raumfahrt, 8031 Oberpfaffenhofen, Federal Republic of Germany.
F. Fanale is with the Institute of Geophysics, University of Hawaii, Honolulu, HI 96822.
C. Anger is with the Institute for Space and Terrestrial Science, Concord, Ontario, Canada L4K 3C8.
M. Carr is with the U.S. Geological Survey, Menlo Park, CA 94025.
C. Pilcher is with NASA Headquarters, Washington, DC 20546.

*To whom correspondence should be addressed.

Among the more than 5000 numbered asteroids, 951 Gaspra is a relatively small, highly elongated, object (*1, 2*) with an average radius of about 7 km (*3*). It orbits near the inner edge of the main asteroid belt (semimajor axis of 2.21 astronomical units) in the so-called Flora region. Its spectral properties observed from Earth place it in the S taxonomic class, the most common asteroid type in the inner half of the asteroid belt (*4, 5*). Surfaces of S-type asteroids are thought to be composed of varying proportions of olivine and pyroxene and iron-nickel metal, but there is debate about whether the S-asteroids are the parent bodies of the common ordinary chondrite meteorites or whether they are geochemically differentiated bodies in which metal segregated from silicates during an early episode of heating and are the sources of the stony-iron meteorites (*6*). A prime goal of Galileo's encounter with Gaspra and the possible encounter in 1993 with another S-type asteroid, 243 Ida, is to study two diverse S-types. Ground-based reflectance spectra show that Gaspra is an unusually red, olivine-rich, S-type, suggesting that it is possibly a fragment of a differentiated body, whereas Ida is a more likely candidate for an ordinary chondrite parent body (*1, 7, 8*).

The Flora region is densely populated with small, S-type asteroids, generally thought to be the fragments of one or more larger precursor asteroids smashed by catastrophic collisions. Gaspra ought to be a collisional fragment, because rocky objects of its size have model lifetimes against collisional destruction much shorter than the age of the solar system (*9–11*).

Appearance, Size, and Shape

Gaspra is revealed to be an irregularly shaped body with a conspicuously cratered surface, but one with a scarcity of craters larger than about 1.5 km in diameter. There are also hints of generally linear features at the limit of resolution (164 m per pixel; phase angle = 39°). The illuminated portion of Gaspra (Fig. 1), about 16 by 12 km, displays an aspect consistent with Earth-based predictions based on light curve analyses, which yield a spin period of 7.04 hours and a spin axis pointing in the